Received: 30 January 2023 | Revised: 27 July 2023 | Accepted: 8 August 2023

DOI: 10.1002/dad2.12477

Alzheimer's & Dementia
Diagnosis, Assessment & Disease Monitoring

RESEARCH ARTICLE

Combining aperiodic 1/f slopes and brain simulation: An EEG/MEG proxy marker of excitation/inhibition imbalance in Alzheimer's disease

Pablo Martínez-Cañada[1,2] | **Eduardo Perez-Valero**[1,2] | **Jesus Minguillon**[2,3] | **Francisco Pelayo**[1,2] | **Miguel A. López-Gordo**[2,3] | **Christian Morillas**[1,2]

[1]Department of Computer Engineering, Automation and Robotics, University of Granada, Granada, Spain

[2]Research Centre for Information and Communications Technologies (CITIC), University of Granada, Granada, Spain

[3]Department of Signal Theory, Telematics and Communications, University of Granada, Granada, Spain

Correspondence
Pablo Martínez-Cañada, Research Centre for Information and Communications Technologies (CITIC), University of Granada, Periodista Rafael Gómez Montero 2, Granada, 18014, Spain.
Email: pablomc@ugr.es

Funding information
Ministerio de Ciencia e Innovación, Gobierno de España/Agencia Estatal de Investigación/European Regional Development Fund, Grant/Award Numbers: PID2022-137461NB-C31, PID2022-139055OA-I00, PID2021-128529OA-I00; Consejería de Universidad, Investigación e Innovación, Junta de Andalucía, Grant/Award Number: PROYEXCEL_00084; Universidad de Granada, Grant/Award Numbers: PPJIA2022.33, PP2022.PP.33, PP2021.PP-28

Abstract

INTRODUCTION: Accumulation and interaction of amyloid-beta (Aβ) and tau proteins during progression of Alzheimer's disease (AD) are shown to tilt neuronal circuits away from balanced excitation/inhibition (E/I). Current available techniques for noninvasive interrogation of E/I in the intact human brain, for example, magnetic resonance spectroscopy (MRS), are highly restrictive (i.e., limited spatial extent), have low temporal and spatial resolution and suffer from the limited ability to distinguish accurately between different neurotransmitters complicating its interpretation. As such, these methods alone offer an incomplete explanation of E/I. Recently, the aperiodic component of neural power spectrum, often referred to in the literature as the '1/f slope', has been described as a promising and scalable biomarker that can track disruptions in E/I potentially underlying a spectrum of clinical conditions, such as autism, schizophrenia, or epilepsy, as well as developmental E/I changes as seen in aging.

METHODS: Using 1/f slopes from resting-state spectral data and computational modeling, we developed a new method for inferring E/I alterations in AD.

RESULTS: We tested our method on recent freely and publicly available electroencephalography (EEG) and magnetoencephalography (MEG) datasets of patients with AD or prodromal disease and demonstrated the method's potential for uncovering regional patterns of abnormal excitatory and inhibitory parameters.

DISCUSSION: Our results provide a general framework for investigating circuit-level disorders in AD and developing therapeutic interventions that aim to restore the balance between excitation and inhibition.

KEYWORDS
1/f slope, Alzheimer's disease, EEG, excitation-inhibition, MEG, network of spiking neurons

1 | INTRODUCTION

Abnormal accumulation and circuit-level interactions of amyloid-beta (Aβ) and tau proteins in the cortex are the neuropathologic hallmarks of Alzheimer's disease (AD), starting decades before the emergence of clinically measurable cognitive deficits.[1–3] Previous findings suggest that neuronal and circuit level modes of dysfunction (i.e., hyper- and hypoexcitability) can arise from the neuronal effects mediated by AD-related proteins. Interestingly, Aβ and tau have shown to exhibit opposing effects on local circuit dynamics. There is strong evidence that Aβ plaques, as well as soluble forms of Aβ, are a key player in driving neuronal hyperexcitability in AD, which might ultimately give rise to epileptiform activity.[4–7] In direct contrast to Aβ-mediated effects, tau is associated with suppression of neuronal activity (hypoexcitability) and progressive loss of connectivity.[8,9] Moreover, Aβ and tau may not act independently; recent evidence suggests that both pathologies have synergistic effects.[1] During AD progression, Aβ and tau show different temporal evolution profiles (in which tau pathology is delayed), are initially deposited in different brain regions (Aβ plaques are particularly found in medial prefrontal and medial parietal regions, while tau aggregates in the medial temporal lobe), and propagate across other cortical regions as the disease progresses.[1–3,10,11] Given the complexity of the competing and synergistic functional effects between AD-related proteins, disambiguating their influence on neural dynamics and identifying how they modulate circuit excitation and inhibition (E/I balance) remains a topic of intense research.[2,12,13]

Direct and indirect in vivo measurement of E/I is especially challenging in the human brain. Current noninvasive assessments of E/I in humans are largely restricted to magnetic resonance spectroscopy (MRS) measurements of in vivo concentrations of primary excitatory (glutamate) and inhibitory (γ-aminobutyric acid, GABA) neurotransmitters.[14–17] This approach presents several methodological challenges: the relatively low signals of glutamate and GABA complicate their interpretation because of their overlap with signals from other metabolites, it has low temporal and spatial resolution, and their measurements are usually restricted to one or few brain regions. For these reasons, current MRS approaches have limited utility for tracking variations of E/I across cortical regions or behavioral states. Recently, a range of novel features derived from electroencephalography (EEG) and magnetoencephalography (MEG) recordings have been described as robust proxy makers for noninvasive real-time measurements of changes in E/I balance.[18–22] One of the most promising candidate E/I biomarkers is the exponent of the 1/f spectral power law, often referred to in the literature as the '1/f slope'. Converging evidence from neuroimaging, pharmacological, chemogenetic, and computational modeling studies has linked changes in this marker to conditions related to altered E/I balance,[23] such as autism,[19,24] schizophrenia,[21] epilepsy,[25,26] and attention-deficit/hyperactivity disorder.[27,28] The 1/f slope has been additionally shown to exhibit strong changes both across healthy aging[29,30] and during early development,[31,32] which have been associated to alterations in the relative E/I ratio.

RESEARCH IN CONTEXT

Systematic review: We conducted a review of PubMed-indexed articles investigating neuroimaging biomarkers that can track disruptions in excitation/inhibition (E/I) potentially underlying Alzheimer's disease (AD). While biomarkers of E/I imbalance are not yet as widely studied as other biomarkers of AD, there have been some recent publications stressing the importance of studying E/I imbalance at the circuit level, which could be the most effective scale for neuroscientific investigation and intervention. These relevant citations are appropriately cited.

Interpretation: Our results support the hypothesis that E/I imbalance in AD is reflected by and thus could be inferred from the readout of spectral slope and demonstrate the potential of this biomarker to be used alone or in combination with other biomarkers to investigate circuit dysfunction in AD models.

Future directions: Recently, a range of novel E/I biomarkers has been described that are noninvasive and applicable in humans and which can be deployed on a large scale. Although each of these markers has been mapped to a different level of neural inference in the brain, they are likely intercorrelated with one another, and potentially estimate overlapping aspects of the same underlying signal at different scales. Further work would be needed to examine the relationship between neural variables measured by each biomarker and to investigate whether they can be used in combination for a more comprehensive interrogation of E/I balance.

Here, we introduce an approach that combines 1/f slopes from resting-state spectral data and simulation of a cortical microcircuit model with recurrent interactions between excitatory and inhibitory neuronal populations[33–35] for inferring E/I alterations in AD. We used our model-based inference approach to interrogate two recent publicly available datasets of EEG[36] and MEG[37] recordings of patients with AD or mild cognitive impairment (MCI). Finally, we assessed the potential of our approach for revealing the specific shifts in E/I occurring across cortical regions distinctively associated with tau and Aβ depositions at different stages of AD.

2 | MATERIALS AND METHODS

2.1 | Participants

We used resting-state EEG and MEG data of people with AD or prodromal disease from open and publicly available datasets. The EEG

dataset[36] included recordings of individuals between the ages of 40 and 90 that were collected at four sites in the United Sates: Advanced Brain Monitoring (ABM) in Carlsbad, California; Advanced Neurobehavioral Health (ANH) in San Diego, California; Massachusetts General Hospital (MGH) in Boston, Massachusetts; and Mayo Clinic (MAYO) in Rochester, Minnesota. Healthy controls were in two age groups: between 40 and 60 (HC2, $n = 62$) and between 60 and 90 (HC3, $n = 52$). Participants in the AD group ($n = 26$) were in the age range of 58 to 90. Patients were diagnosed with AD according to neurological evaluation and neuropsychological testing based on criteria developed by the National Institute of Neurological and Communicative Disorders and Stroke and the Alzheimer's Disease and Related Disorders Association (NINCDS-ADRDA)[38] and based on the Diagnostic and Statistical Manual of Mental Disorders (DSM-5) criteria for major neurocognitive disorder (i.e., dementia) due to AD. Participants were excluded if they reported known neurological or psychiatric disorders, cardiac arrhythmias, heart failure (e.g., myocardial infarction), epilepsy, HIV+ diagnosis, bipolar disorder, or major depression (see ref. 36 for more details).

MEG data were acquired from the BioFIND project,[37] which included individuals with clinically diagnosed MCI and healthy controls pooled over a number of different projects from two sites: the MRC Cognition & Brain Sciences Unit (CBU) in Cambridge, England, and the Centre for Biomedical Technology (CTB) in Madrid, Spain. The MCI diagnosis of patients from CBU included Addenbrooke's Cognitive Examination (ACE) and ACE Revised (ACE-R), and Mini Mental State Examination (MMSE) tests as standard. Positron emission tomography (PET) and fluidic biomarkers were not performed to patients, although magnetic resonance imaging (MRI) was used for clinical follow-up in support of the diagnosis. Controls from CBU were selected from the population-derived CamCAN[39] cohort of healthy people from the same geographic region and having similar age and sex distribution. Controls were diagnosed based on MMSE (and indeed ACE-R) scores above conventional cutoffs. The MCI diagnosis of patients from CTB was determined with intermediate probability according to the National Institute on Aging-Alzheimer Association criteria[40] that is given by a clinician based on clinical and cognitive tests, self- and informant-report, and in the absence of full dementia or obvious other causes. For some patients, there was additional biomarker evidence of atrophy from MRI or long-term follow-up and genotyping for the apolipoprotein E (APOE) $\varepsilon 4$ allele. The CTB controls had a full neuropsychological assessment to confirm normal cognition, and the same type of biomarker assessment as that done for the MCI group. For a subset of MCI patients, additional information was provided indicating whether or not they subsequently progressed to dementia ("probable AD") over subsequent years, according to their managing clinician. We only used MCI patients from this subset so that our results can be interpreted in terms of neural changes associated with probable AD (converted) or with patients who later did not convert to a dementia diagnosis (not converted). Additionally, and provided that age is the most important risk factor for developing AD,[2,13] we limited our study of the BioFIND dataset to elder individuals (older than 75 years), including $n = 50$ MCI patients ($n = 27$ converted, $n = 23$ not converted) and $n = 51$ controls.

2.2 | Preprocessing and power spectral analysis

We used the same preprocessing methods as described in the respective publications of the MEG and EEG datasets.[36,37] We refer the reader to the corresponding publications for a detailed description of the preprocessing steps.

Briefly, EEG and MEG recordings were gathered during resting state with eyes closed (during 5 minutes for EEG recordings and 481.5 and 180 seconds for controls and MCI in MEG recordings) and band-pass filtered (1-49 Hz for EEG data and from 0.5 to 48 Hz for MEG data). Bad channels of EEG data were detected and removed, as well as sources other than brain, for example, eye blinks (less than 0.01% of total data were excluded). EEG data were then epoched into 1-second non-overlapping windows at each channel. The first step of the MEG analysis pipeline included Signal Space Separation (SSS) using MaxFilter version 2.2.12.[41] The full parameters used by MaxFilter are described in the corresponding publication.[37] Briefly, in the first call to MaxFilter, the MaxFilter's "autobad" option was used to detect bad channels and MaxFilter's "headpos" option to estimate head position every second. In the second call, MaxFilter was passed the list of channels that were bad in more than 5% of buffers for a given participant before carrying out SSS. Other parameters, such as MaxFilter's "temporal" SSS option, MaxFilter's "mvcomp" and MaxFilter's "trans" option were not used. The other steps of the MEG preprocessing included epoching (2-second window), bad epoch detection (number of bad epochs = 4.1 and 4.7 for controls and MCI), beamforming and region-of-interest (ROI) extraction (further details can found in ref. 37).

EEG power spectral densities (PSD) were available out of the box in the EEG dataset.[36] EEG PSDs were computed using LabX EEG processing software (Advanced Brain Monitoring Inc., Carlsbad, California). LabX employs modified periodogram PSD estimates with a 1-second-long Kaiser window (b = 6) and 50% overlap (see ref. 36 for further details). We computed MEG PSDs of ROIs by ourselves using a similar approach. MEG PSDs were defined by time averaging spectrograms computed with a 1-second-long Kaiser window (b = 6) and 50% overlap. We normalised PSDs by dividing each EEG channel's or ROI's PSD by its mean power.

We parameterized power spectra into periodic and aperiodic components using the FOOOF algorithm[42] with the following configuration: frequency range = (1, 40) Hz, maximum number of peaks = 3, peak threshold = 1, peak width limits = (2, 50) Hz. In this study, we disregarded the periodic (oscillatory) properties of spectral fittings. Aperiodic activity is described by a $1/f^{\chi}$ distribution, with exponentially decreasing power across increasing frequencies. When measured in the log-log space, the χ parameter, referred to as the aperiodic component, is computed as the negative slope of the log-log power spectrum (1/f slope). The aperiodic component is additionally parameterized with an "offset" parameter, which reflects a shift of power

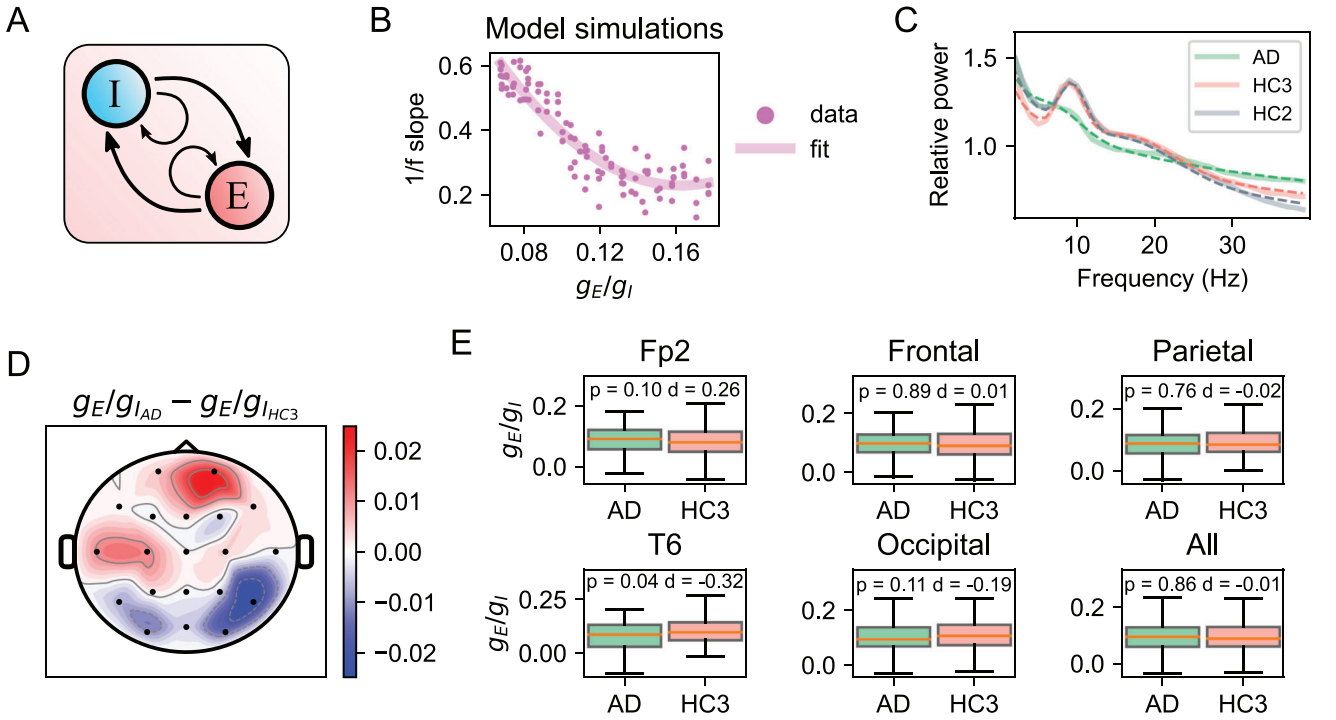

FIGURE 1 Changes of spectral properties in AD and E/I imbalance predictions from the recurrent network model. (A) Overview of the network model that includes recurrent connections between two types of populations: excitatory cells (E) and inhibitory cells (I). (B) 1/f slopes from model simulations as a function of the ratio between synaptic conductances (g_E/g_I) and fit of the polynomial regression model. (C) Normalized power spectrum across all individuals from the HC2, HC3, and AD groups and over all electrode locations. Dash lines correspond to spectral fits including aperiodic and periodic components. (D) Topographic representation of mean differences in g_E/g_I. (E) Predictions of changes in g_E/g_I for specific subsets of electrodes (p and d indicate *p*-value of the two-sided t-test and Cohen's effect size, respectively).

spectrum. Since power spectrum normalization modifies relative differences in the offset of power spectrum, we did not include this parameter in our study to avoid misinterpretation of results.

2.3 | Cortical network model and computation of field potentials

The cortical network model included an excitatory and an inhibitory population of leaky integrate-and-fire (LIF) spiking neuron models that interact through recurrent connections[24,33,34,43] (Figure 1A). Each population received two different Poisson signals: an external input with constant-rate (υ_0) that can represent sensory or cortico-cortical inputs, and a noise input that captures intracortical fluctuations of neural activity. We used the same network configuration with the same parameters as described in previous publications.[24,33,44] Briefly, the network consists of 5000 conductance-based LIF neuron models, 80% of which are excitatory (i.e., they form α-Amino-3-hydroxy-5-methyl-4-isoxazole propionic acid (AMPA)-like excitatory synapses with other neurons) and 20% are inhibitory (forming GABA-like synapses). Neurons in the network are randomly connected with each other (connection probability = 0.2). To account for neural activity with different E/I ratios, we performed several simulations of the recurrent network model where we systematically varied the ratio between excitatory and inhibitory synaptic conductances (g_E/g_I) across the range 0.06 – 0.2 (Figure 1B). We additionally set υ_0 = 3 spikes/s, a low input strength that drives the network into a spontaneous activity regime. We repeated simulations for a given value of g_E/g_I with different random initial conditions (e.g., recurrent connections of the network). All simulations were performed using NEST v2.16.0[45] and parallelized in a high-performance computing server (32-core CPU and 128 GB RAM).

Field potentials cannot be directly computed from LIF neuron models because in a LIF model all transmembrane currents collapse into a single point in space and the resulting extracellular potential (and in turn, the resulting field potential) is zero. An approximation of field potentials can be calculated using variables available from simulation of the network model (e.g., synaptic currents). Here we computed an approximation of M/EEG signals as the sum of absolute values of AMPA and GABA postsynaptic currents on excitatory cells ($\sum |I_{AMPA}| + \sum |I_{GABA}|$). This simple approach was shown to perform remarkably well in predicting simulated field potentials at different spatial scales, from local field potentials (LFPs)[34] to EEGs[33] and in capturing more than 90 % of variance of empirical data recorded in neocortex.[35,46]

2.4 | Regression model for estimating E/I ratio and statistical tests

We computed a least-squares polynomial regression model (degree = 2) with data from the whole set of simulations of the

recurrent neural network (varying g_E/g_I across the range 0.06 – 0.2 and υ_0 = 3 spikes/s). The regression model was computed using x = 1/f slopes from simulated field potentials and y = g_E/g_I values. Estimated parameters of the regression model were used to predict changes in g_E/g_I from slopes of empirical M/EEG data. Measures of slopes and predictions of g_E/g_I followed a normal distribution and had equal variances. We determined whether there was a significant difference between two groups of measures (e.g., control vs. AD) using a two-sided t test. Significant effects between more than two groups of measures (e.g., control, MCI converted and non-converted) were tested using a one-way analysis of variance (ANOVA) test and post-hoc pairwise comparisons with Tukey honestly significant difference (HSD) confidence intervals (alpha = 0.05). We used Cohen's d to account for effect size. In all statistical tests, data were pooled over all epochs and individuals.

3 | RESULTS

3.1 | Opposing E/I shifts in posterior and anterior cortical areas of patients with AD

We first investigated whether variations in spectral slopes could be related to changes in E/I using computational modeling. We performed several simulations of a LIF neural network model with interacting excitatory and inhibitory neuronal populations[24,33,34] (Figure 1A) in which we systematically varied the ratio between synaptic conductances (g_E/g_I) (Figure 1B). From this model, we computed the network's M/EEGs as the sum of absolute values of all synaptic currents, an approximation that has demonstrated to capture the main properties of field potentials at different spatial scales and has been validated on both simulated and real cortical data.[33–35,46] Consistent with previous work,[22,24] 1/f slopes computed from simulated field potentials decreased (flatter slopes) with increasing g_E/g_I. Using simulation data, we computed a polynomial regression model to fit the relationship between g_E/g_I and slope values ($R^2 = 0.77$, $p < 0.001$, Figure 1B). These modeling results indicate that changes in synaptic E/I ratio are reflected by and thus could be potentially inferred from the readout of spectral slope.

We next analyzed EEG data from an open EEG dataset[36] that included resting-state EEG recordings of healthy individuals across different ages (HC2 and HC3 groups) and patients with AD. Comparing power spectra of AD patients and age-matched controls (HC3), we found that spectral recordings of AD patients displayed, as described in various studies (for review, see[13]), slower brain oscillatory activity with a prominent reduction of alpha (8–12 Hz) and beta (12–30 Hz) rhythms, and increased delta/theta (0.5 – 8 Hz) band activity (Figure 1C). Additionally, we observed a flattening of power spectrum in HC3 (older) individuals (Figure 1C), as well as smaller slopes (Figure S1A), compared to HC2 (younger) group, which was consistent with the hypothesis of increasing neural noise in healthy aging.[29,30]

To test whether slopes can be used to predict changes in E/I, we computed 1/f slopes of individuals in AD and HC3 groups and used the regression model to produce g_E/g_I predictions from these empirical slope measures. The topographic representation of changes in g_E/g_I (Figure 1D) revealed an interesting pattern in AD with opposing effects suggesting a coexistence of excitation- and inhibition-dominated regions. This is consistent with Aβ and tau effects at advanced stages of the disease, in which Aβ and tau pathologies are coestablished and coexist.[2] Importantly, we compared local differences in g_E/g_I across subsets of electrodes (Figure 1E) and found that some regions, such as prefrontal locations (Fp2), exhibited stronger shifts in g_E/g_I toward excitation ($p = 0.1$, $d = 0.26$) compared to other locations (but not significant), while g_E/g_I in temporal electrode locations (T6) showed significant shifts toward inhibition ($p = 0.04$, $d = -0.32$). Differences in g_E/g_I between AD patients and controls were much weaker and insignificant when pooling data from all electrode locations (All, Figure 1E), which suggests that local synaptic excitatory and inhibitory drives cancelled each other out at the global network level. Direction and strength of changes in slopes (Figure S1B and C) were largely in agreement with the patterns of differences in g_E/g_I but less prominent at Fp2 and T6 electrode locations.

3.2 | Cortex-wide hyperexcitability in MCI patients

We examined MEG data from a different publicly available dataset, the BioFIND dataset.[37] This dataset included resting-state MEG data of MCI patients and healthy controls. Additional labels were provided for MCI patients indicating whether they subsequently progressed to probable AD (converted) or did not convert to a dementia diagnosis (not converted). We computed average MEG power spectra and found substantial differences in spectral properties between controls (Ctrl) and MCI patients (Figure 2A). Power spectrum shapes of controls and not-converted MCI patients (MCI_n) largely overlapped across a broadband of low frequencies from 0.5 to 12 Hz. In contrast, the power spectrum of converted MCI patients (MCI_{cv}) comparatively captured some of the defining features of AD at lower frequencies, such as attenuation of alpha rhythm and increased delta/theta power. At higher frequencies (> 25 Hz), power spectra of MCI_n and MCI_{cv} eventually converged and showed higher power than control spectra.

We then computed 1/f slopes (Figure S3) and their corresponding g_E/g_I estimates (Figure 2B and C, and Figure S2) for every one of the 38 ROIs of the parcellation used here (described in ref. 47). Hyperexcitability (i.e., increased g_E/g_I) ostensibly dominated along cortical regions in both MCI groups and agreed with clinical data of Aβ hyperactivity in early AD.[2] Consistently, slopes of MCI_n and MCI_{cv} were overall reduced across ROIs (Supp. Figure 3). The analysis of g_E/g_I predictions pooled across all ROIs (All, Figure 2C) revealed statistically significant global differences between controls and MCI_n, and between controls and MCI_{cv} ($p < 0.001$ in both cases) although small size effects ($d \leq 0.17$). We finally compared regional g_E/g_I variations across subsets of ROIs (R1, R2, R3, and R4, Figure 2C) and observed that most g_E/g_I shifts of MCI_{cv} with respect to controls were insignificant or marginally significant, while g_E/g_I variations between MCI_n and controls were overall stronger and significant ($p < 0.01$, $d \geq 0.2$ in all subsets of ROIs). The

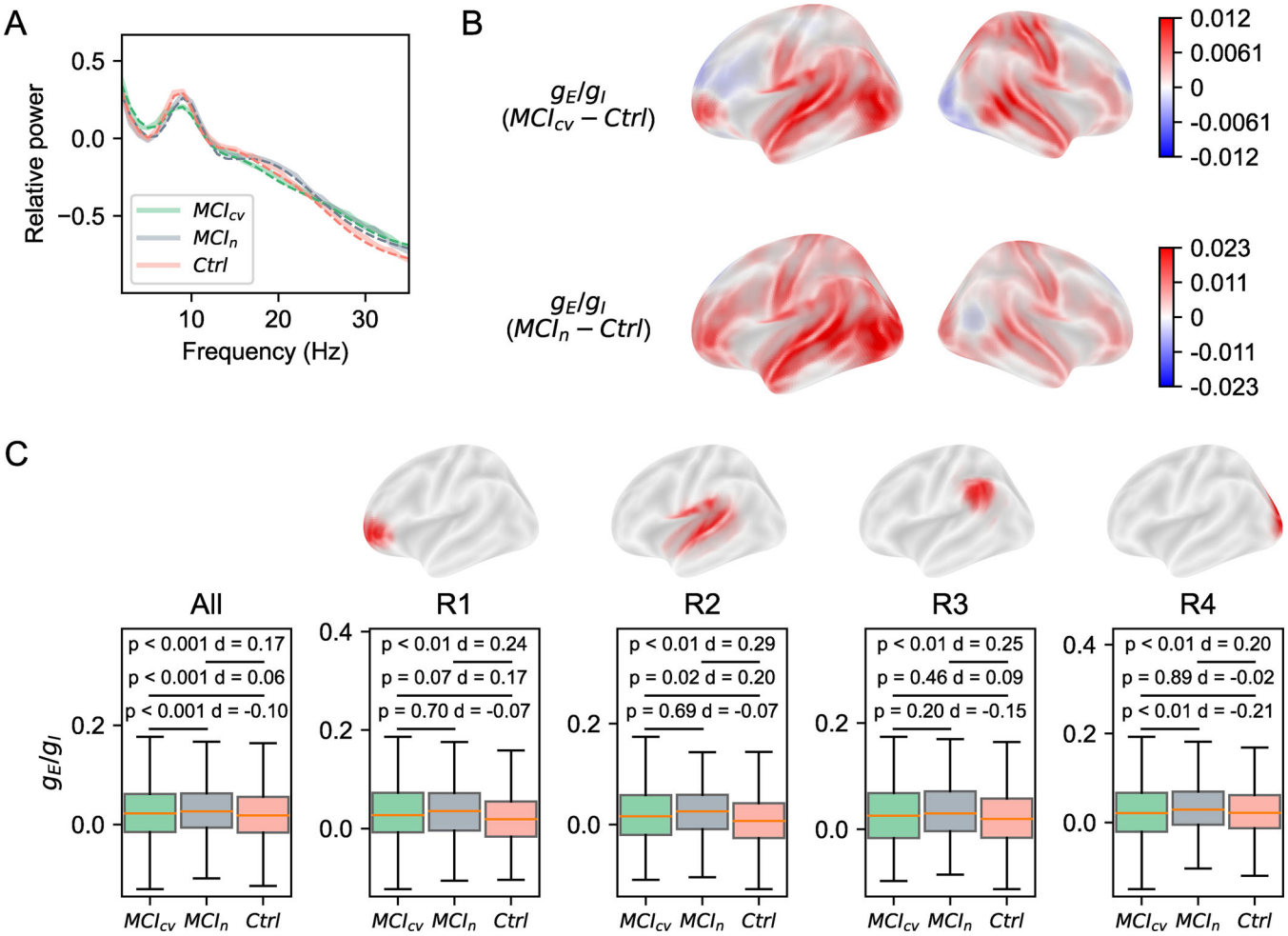

FIGURE 2 Spectral changes and E/I shifts in MCI. (A) Normalized power spectrum across all individuals from the control (Ctrl), MCI_n, and MCI_{cv} groups and over all ROIs. (B) Surface plots (lateral view) representing mean differences in g_E/g_I. (C) Predictions of g_E/g_I pooled across all ROIs (All), and for a subset of selected ROIs (R1, R2, R3 and R4) represented in the upper surface plots (p and d indicate *p*-value of the post-hoc Tukey HSD test and Cohen's effect size respectively).

weaker increase in local and global excitability of MCI converters may be linked to the presence of inhibitory influences that may reflect a more advanced stage of the disease and the onset of tau pathology.

4 | DISCUSSION

We have described a new method for inferring alteration in the E/I balance of neuronal circuits in AD using EEG and MEG measures. It is based on a recent neuroimaging biomarker, the 1/f slope, which has been proposed as a robust proxy marker for noninvasive real-time interrogation of E/I imbalance in many neuropsychiatric conditions.[18] We used a regression model to map empirical 1/f slopes onto E/I estimations obtained from computational simulations of a recurrent cortical microcircuit model of spiking neurons that has shown to capture the main properties of simulated and real field potentials.[24,33,34] We evaluated the ability of our approach to identify potential E/I imbalances using recordings of patients at prodromal and clinical stages from publicly available EEG[36] and MEG[37] datasets. Collectively, our results support the hypothesis that E/I imbalance in AD is reflected by and thus could be inferred from the readout of spectral slope and demonstrate the potential of this biomarker to be used to investigate circuit dysfunction in AD models. We discuss the implications and limitations of our method below.

4.1 | Predictions of E/I imbalances are potentially associated with spatiotemporal progression of tau and Aβ in AD pathophysiology at circuit level

Aβ and tau dynamically modulate neuronal and circuit activity during AD progression.[1,2,10,13,48] At earlier stages, Aβ plaques accumulate and predispose neuronal circuits toward neuronal hyperexcitability (Figure 3). Importantly, epileptic activity and enhanced seizure susceptibility are phenomena often observed in early AD.[49,50] A key finding from the current study is consistent with these observations. We found that E/I prediction results from the cohort of patients with MCI, a prodromal state of AD (likely between early and mid stages in Figure 3),

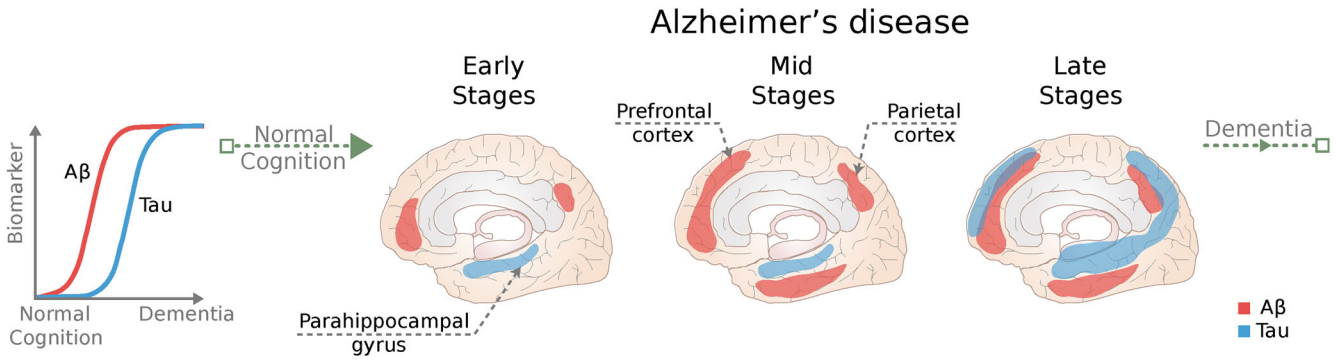

FIGURE 3 Schematic representation of the spatiotemporal progression of Aβ and tau biomarker levels during AD progression. As the disease progresses, Aβ and tau show different temporal evolution profiles in which Aβ plaque deposition precedes cortical tau pathology. Aβ and tau pathologies initially start in different brain regions. Aβ plaques are initially deposited in medial prefrontal and medial parietal regions, while tau aggregates first become evident in the medial temporal lobe, probably starting in the entorhinal cortex. During AD progression, Aβ and tau spread through different areas of cortex and may interact synergistically. Blue and red shaded areas indicate the areas affected by tau and Aβ pathology, respectively. This schematic plot was created based on refs. 1, 2, 10, 11

consistently displayed a generalized pattern of hyperexcitability along cortical regions. Tau pathology, which is primarily associated with suppression of neuronal activity, by contrast, becomes evident in later stages of AD progression, at advancing disease stages.[10] Indeed, it has been shown that increase in tau pathology correlates much more strongly than Aβ pathology with neurodegeneration and cognitive impairment, the hallmarks of the clinical stage of AD. The tau aggregates are commonly found in the medial temporal lobe, starting in the parahippocampal gyrus, which includes the entorhinal cortex, from which they spread to limbic areas, and from there to the association areas.[1] At advanced stages of the disease, thus, Aβ and tau pathologies coexist and interact, and their effects, in combination, can shift neuronal circuits from balanced E/I toward hyperexcitability or hypoexcitability. Our findings based on E/I estimations using EEG data from patients with AD draw remarkable potential parallels to the spatiotemporal evolution profiles of Aβ and tau between probably occurring at mid and late stages (Figure 3). First, topographic representation of E/I estimates revealed a coexistence of excitation- and inhibition-dominated regions. Second, we found significant patterns of hyperexcitability in prefrontal locations (regions associated with initial Aβ deposition) and of hypoexcitability in the temporal lobe (associated with initial tau accumulation). Taken together, these results show the potential of our inference method to track E/I disruptions during AD progression both spatially and over time.

4.2 | Impact of our method to investigate brain dysfunction at the circuit level and monitor responses to drug treatments that aim to restore the balance between excitation and inhibition

A leading theory holds that many neurodevelopmental disorders, from autism to schizophrenia, and neurodegenerative diseases, such as AD, are the result of an imbalance in the activity of excitatory and inhibitory neurons.[2,13,51–54] Brain dysfunction has been traditionally investigated and diagnosed entirely at the behavioral level, whereas interventions aimed to correct alterations pharmacologically focused on the molecular level. A recent viewpoint argues that the most effective scale for neuroscientific investigation and intervention could be the circuit level,[2,3,13,51] which is the intermediary scale bringing the gap between molecular and genetic changes at the microscopic level and macroscopic alterations in behavior. Our modeling approach provides a mechanistic framework linking abnormal E/I ratio at the level of circuits (where neuronal and synaptic changes mediated by AD-related proteins possibly converge) to properties of macroscopic brain signals (M/EEG). Results of this study indicate that computational modeling at the circuit level could help integrate neurophysiological aspects of AD at the micro-, meso-, and macroscale. Moreover, we have shown that our inference method largely tracks directionality of expected E/I shifts during AD progression; thus, our approach could be used to estimate changes in excitatory and inhibitory circuit parameters in response to administration of pharmacological drugs commonly used for treatment of different clinical disorders (e.g., memantine, ketamine, or lorazepam).

4.3 | Novel noninvasive E/I proxy markers

Recently, a range of novel E/I biomarkers has been described that are noninvasive and applicable in humans and that can be deployed on a large scale.[18] These markers represent a key translational link across species and recording scales and can be applied in resting-state experiments and tasks that do not require extensive cognitive processing. They have been used to make inferences of E/I disruptions across many psychiatric and neurodevelopmental disorders, often combined with pharmacological or chemogenetic manipulations that modulate the level of inhibition and excitation,[19,21,24] or to uncover the neural circuit basis of some key brain processes such as development[31,32] or aging.[29,30] Some of these novel E/I markers are aperiodic 1/f signal,[22,24] neuronal avalanches,[55,56] long-range

temporal correlations (LRTC),[57] neural entropy,[58,59] and microstates.[60] Although each of these markers has been mapped to a different level of neural inference in the brain, they are likely intercorrelated with one another, and potentially estimate overlapping aspects of the same underlying signal at different scales. Further work would be needed to examine the relationship between neural variables measured by each biomarker and to investigate whether they can be used in combination for a more comprehensive interrogation of E/I balance. Additionally, combining these biomarkers with other imaging techniques, such as MRS and PET,[12,61,62] will allow us to gain a better insight into the mechanisms of E/I by leveraging the strengths of each method.

4.4 | Biophysical modeling in AD research

Previous models in AD research have lumped neural populations at each brain region into neural masses (neural mass models).[12,63–68] Using neural mass models, recent studies have found a relationship between abnormal excitatory and inhibitory time-constants and spatial depositions of Aβ and tau,[12,66] have linked neuronal hyperactivity in preclinical AD to oscillatory slowing,[64,66] and have developed a successful strategy to preserve network integrity during AD progression.[68] A recent work has also used neural mass models to extract information about the excitatory/inhibitory balance in single subjects and suggested that AD subjects were characterized by increased global coupling and increased inhibition.[63]

Neural mass models have been proven useful to explain large-scale neuronal processes and structure-function coupling at macroscopic scales. Spiking and multicompartment models rather focus on describing neural phenomena at the micro- and mesoscopic scales and allow researchers to simulate synaptic connectivity, individual spike events and/or whole-cell dynamics, as well as heterogeneous parameter distributions in network populations. Due to limited computational resources and the higher level of complexity of point neuron models and especially multicompartment models, appropriateness and interpretability of these models at whole-brain scale has been questioned. However, these models are uniquely positioned at an intermediary scale of biophysical description, which facilitates interpretation of the relationship between neuronal and synaptic changes mediated by molecular and cellular mechanisms with circuit-level dynamics and properties of field potentials. Moreover, a range of studies have developed biophysics-based methods for computing "proxies" of field potentials that provide accurate approximations of extracellular signals from simulations of spiking network models.[33,34,69,70] Recently, large-scale network models of cortex incorporating point neuron or multicompartment models and data-driven long-range connectivity between areas have shown to reproduce both experimental spiking statistics and cortico-cortical interaction patterns measured in functional MRI.[71,72] Spiking and multicompartment models offer a new perspective for unifying local and large-scale accounts of cortical dynamics and provide a promising platform for future studies of brain function and dysfunction.

4.5 | Limitations and future work

Our findings should be considered in the context of the following limitations. Our approach is based on a spiking network model of recurrently connected excitatory and inhibitory neuronal populations that has been constructed to approximate circuit phenomena with high accuracy at the local scale level.[35,44,73,74] However, we did not model brain structure and function at the scale of macroscopic networks, that is, among brain regions and their long-range cortico-cortical connections. Mean field or neural mass models[75–78], coupled using anatomic connectivity information, have been employed to account for whole-brain macroscopic phenomena, such as the emergence of patterns of coherent activity across regions in the cerebral cortex and propagation of slower oscillatory rhythms. The most effective scale for studying AD (and other clinical conditions) and for intervention remains an area of active research.[2,13] The challenge for future research on neural functional impairment will be to devise and implement the necessary multilevel computational modeling approaches that can integrate local circuitry and long-range circuit dynamics.[71,72,79]

Another limitation of our approach is that the cortical circuit model in its current form does not include some important synaptic mechanisms such as N-methyl-D-aspartate (NMDA) synapses. NMDA receptors are critically involved in persistent cortical activity underlying working memory and evidence accumulation.[79,80] Disruptions in cortical NMDA receptor signalling have been associated with certain brain disorders, including AD,[81] and likely affect E/I balance.[21,82–84] Using our simplified model of recurrent AMPA and GABA synaptic currents, we have demonstrated here that E/I imbalances across cortical regions can be consistently associated to spatiotemporal evolution profiles of AD-related proteins. An interesting topic for a future study would be to extend the spiking network model to include NMDA synapses and to assess their impact on the current prediction results of E/I alterations in AD.

The range of frequencies used to fit the aperiodic component of power spectrum varies across studies.[21,22,24,30] A recent study that investigated E/I changes in AD has also incorporated the aperiodic exponent of power spectrum as a proxy marker to determine differences in E/I balance.[85] Using a range of frequencies between 30 and 48 Hz, they observed a lower aperiodic exponent (a shift of E/I toward excitation) in AD dementia patients. Future studies should methodically quantify how the E/I ratio changes as a function of the range of frequencies employed and identify the most appropriate frequency range to compute the 1/f slope that could produce the most accurate estimates of E/I imbalances in AD.

Finally, it is noteworthy to mention that the experimental protocols for recording the open EEG and MEG data used in this study and for recruiting participants, though they are out of our control, include additional limitations. First is the fact that the data come from different sites. Although the recording machine models were identical, there are still differences in individual devices (e.g., in their noise level). The clinical assessments followed international guidelines but the precise categorization as AD, MCI, and control is likely to differ across clinicians at different sites. The tasks performed prior to

resting were different and likely had different levels of fatigue, which could have contributed to noise in the data. The groups also differ in other respects, such as age and education.

5 | CONCLUSION

A prominent view is that circuit-level effects mediated by AD-related proteins provide diagnostic and prognostic information and offer a unique framework to understand AD and develop effective therapeutic interventions. Disambiguating the complexity of Aβ and tau excitatory and inhibitory influences and their interacting effects at the synaptic and circuit scales will be a crucial next step to identify rational therapeutic targets in AD. The approach presented here, consisting of recurrent network modeling and multimodal neuroimaging data, provides a general framework for investigating circuit-level excitatory/inhibitory imbalances and could help in linking micro- and macroscopic scales of investigation in AD.

AUTHOR CONTRIBUTIONS

Pablo Martínez-Cañada: Conceptualization, Methodology, Formal analysis, Software, Writing—original draft, Writing—review & editing, Funding acquisition; **Eduardo Perez-Valero**: Methodology, Writing—review & editing, Funding acquisition; **Jesus Minguillon**: Methodology, Writing—review & editing, Funding acquisition; **Francisco Pelayo**: Methodology, Writing—review & editing, Funding acquisition; **Miguel A. López-Gordo**: Methodology, Writing—review & editing, Resources, Funding acquisition; **Christian Morillas**: Methodology, Writing—review & editing, Resources, Funding acquisition.

ACKNOWLEDGMENTS

We thank members of the NeuroEngineering and Computing (NECo) Lab (University of Granada, Spain) for their invaluable discussions and feedback on this work. This work was conducted using the MRC Dementias Platform UK (DPUK). DPUK is a Public Private Partnership funded by the Medical Research Council (MR/L023784/1 and MR/009076/1). For further information on this resource visit www.dementiasplatform.uk. This project has received funding from MCIN / AEI / 10.13039/501100011033 / FEDER, EU (grants PID2022-137461NB-C31 to C.M., PID2022-139055OA-I00 to P.M.C. and PID2021-128529OA-I00 to M.A.L.G.), from "Junta de Andalucía"—Postdoctoral Fellowship Programme PAIDI 2020 (to J.M.) and 2021 (to P.M.C.), from "Junta de Andalucía"—Projects for Excellence Research (grant PROYEXCEL_00084 to M.A.L.G.) and from University of Granada – "Plan Propio de Investigación" 2021 and 2022 (grant PPJIA2022.33 to P.M.C. and J.M., PP2022.PP.33 to J.M. and PP2021.PP-28 to M.A.L.G). The funders did not play any role in the study design, data collection and analysis, decision to publish, or preparation of the manuscript.

CONFLICT OF INTEREST STATEMENT

Author disclosures are available in the supporting information.

DATA AVAILABILITY STATEMENT

Code used to compute 1/f slopes and E/I predictions, as well as code supporting the findings of this study can be found at https://github.com/pablomc88/EEG-and-MEG-Proxy-Marker-of-Excitation-Inhibition-Imbalance-in-Alzheimer-s-Disease. The EEG dataset was downloaded from Mendeley Data and is accessible via the following DOI: 10.17632/wttpypkctg.2. The MEG dataset used in this study is available on request from the Dementia Platform UK (DPUK) (https://portal.dementiasplatform.uk/Apply).

CONSENT STATEMENT

Consent of human subjects was not necessary.

ORCID

Pablo Martínez-Cañada https://orcid.org/0000-0003-2634-5229

REFERENCES

1. Busche MA, Hyman BT. Synergy between amyloid-β and tau in Alzheimer's disease. *Nat Neurosci*. 2020;23(10):1183-1193. doi: 10.1038/s41593-020-0687-6
2. Harris SS, Wolf F, De Strooper B, Busche MA. Tipping the scales: peptide-dependent dysregulation of neural circuit dynamics in Alzheimer's disease. *Neuron*. 2020;107(3):417-435. doi: 10.1016/j.neuron.2020.06.005
3. Palop JJ, Mucke L. Network abnormalities and interneuron dysfunction in Alzheimer disease. *Nat Rev Neurosci*. 2016;17(12):777-792. doi: 10.1038/nrn.2016.141
4. Zott B, Simon MM, Hong W, et al. A vicious cycle of β amyloid-dependent neuronal hyperactivation. *Science*. 2019;365(6453):559-565. doi: 10.1126/science.aay0198
5. Busche MA, Kekuš M, Adelsberger H, et al. Rescue of long-range circuit dysfunction in Alzheimer's disease models. *Nat Neurosci*. 2015;18(11):1623-1630. doi: 10.1038/nn.4137
6. Verret L, Mann EO, Hang GB, et al. Inhibitory interneuron deficit links altered network activity and cognitive dysfunction in Alzheimer model. *Cell*. 2012;149(3):708-721. doi: 10.1016/j.cell.2012.02.046
7. Busche MA, Eichhoff G, Adelsberger H, et al. Clusters of hyperactive neurons near amyloid plaques in a mouse model of Alzheimer's disease. *Science*. 2008;321(5896):1686-1689. doi: 10.1126/science.1162844
8. Busche MA, Wegmann S, Dujardin S, et al. Tau impairs neural circuits, dominating amyloid-β effects, in Alzheimer models in vivo. *Nat Neurosci*. 2019;22(1):57-64. doi: 10.1038/s41593-018-0289-8
9. Green C, Sydow A, Vogel S, et al. Functional networks are impaired by elevated tau-protein but reversible in a regulatable Alzheimer's disease mouse model. *Mol Neurodegener*. 2019;14(1):13. doi: 10.1186/s13024-019-0316-6
10. van der Kant R, Goldstein LSB, Ossenkoppele R. Amyloid-β-independent regulators of tau pathology in Alzheimer disease. *Nat Rev Neurosci*. 2020;21(1):21-35. doi: 10.1038/s41583-019-0240-3
11. Leuzy A, Chiotis K, Lemoine L, et al. Tau PET imaging in neurodegenerative tauopathies-still a challenge. *Mol Psychiatry*. 2019;24(8):1112-1134. doi: 10.1038/s41380-018-0342-8
12. Ranasinghe KG, Verma P, Cai C, et al. Altered excitatory and inhibitory neuronal subpopulation parameters are distinctly associated with tau and amyloid in Alzheimer's disease. *Elife*. 2022;11:e77850. doi: 10.7554/eLife.77850
13. Maestú F, de Haan W, Busche MA, DeFelipe J. Neuronal excitation/inhibition imbalance: core element of a translational perspective on Alzheimer pathophysiology. *Ageing Res Rev*. 2021;69:101372. doi: 10.1016/j.arr.2021.101372

14. Cuypers K, Marsman A. Transcranial magnetic stimulation and magnetic resonance spectroscopy: opportunities for a bimodal approach in human neuroscience. *Neuroimage*. 2021;224:117394. doi: 10.1016/j.neuroimage.2020.117394
15. Rideaux R. No balance between glutamate+glutamine and GABA+ in visual or motor cortices of the human brain: a magnetic resonance spectroscopy study. *Neuroimage*. 2021;237:118191. doi: 10.1016/j.neuroimage.2021.118191
16. Steel A, Mikkelsen M, Edden RAE, Robertson CE. Regional balance between glutamate+glutamine and GABA+ in the resting human brain. *Neuroimage*. 2020;220:117112. doi: 10.1016/j.neuroimage.2020.117112
17. Stanley JA, Raz N. Functional magnetic resonance spectroscopy: the "New" MRS for cognitive neuroscience and psychiatry research. *Front Psychiatry*. 2018;9:76. doi: 10.3389/fpsyt.2018.00076
18. Ahmad J, Ellis C, Leech R, et al. From mechanisms to markers: novel noninvasive EEG proxy markers of the neural excitation and inhibition system in humans. *Transl Psychiatry*. 2022;12(1):467. doi: 10.1038/s41398-022-02218-z
19. Manyukhina VO, Prokofyev AO, Galuta IA, et al. Globally elevated excitation-inhibition ratio in children with autism spectrum disorder and below-average intelligence. *Mol Autism*. 2022;13(1):20. doi: 10.1186/s13229-022-00498-2
20. Martínez-Cañada P, Noei S, Panzeri S. Methods for inferring neural circuit interactions and neuromodulation from local field potential and electroencephalogram measures. *Brain Informatics*. 2021;8(1):27. doi: 10.1186/s40708-021-00148-y
21. Molina JL, Voytek B, Thomas ML, et al. Memantine effects on electroencephalographic measures of putative excitatory/inhibitory balance in schizophrenia. *Biol Psychiatry Cogn Neurosci Neuroimaging*. 2020;5(6):562-568. doi: 10.1016/j.bpsc.2020.02.004
22. Gao R, Peterson EJ, Voytek B. Inferring synaptic excitation/inhibition balance from field potentials. *Neuroimage*. 2017;158:70-78. doi: 10.1016/j.neuroimage.2017.06.078
23. Pani SM, Saba L, Fraschini M. Clinical applications of EEG power spectra aperiodic component analysis: a mini-review. *Clin Neurophysiol*. 2022;143:1-13. doi: 10.1016/j.clinph.2022.08.010
24. Trakoshis S, Martínez-Cañada P, Rocchi F, et al. Intrinsic excitation-inhibition imbalance affects medial prefrontal cortex differently in autistic men versus women. *Elife*. 2020;9:e55684. doi: 10.7554/eLife.55684
25. van Heumen S, Moreau JT, Simard-Tremblay E, Albrecht S, Dudley RW, Baillet S. Case report: aperiodic fluctuations of neural activity in the Ictal MEG of a child with drug-resistant fronto-temporal epilepsy. *Front Hum Neurosci*. 2021;15:646426. doi: 10.3389/fnhum.2021.646426
26. Pani SM, Fraschini M, Figorilli M, Tamburrino L, Ferri R, Puligheddu M. Sleep-related hypermotor epilepsy and non-rapid eye movement parasomnias: differences in the periodic and aperiodic component of the electroencephalographic power spectra. *J Sleep Res*. 2021;30(5):e13339. doi: 10.1111/jsr.13339
27. Karalunas SL, Ostlund BD, Alperin BR, et al. Electroencephalogram aperiodic power spectral slope can be reliably measured and predicts ADHD risk in early development. *Dev Psychobiol*. 2022;64(3):e22228. doi: 10.1002/dev.22228
28. Robertson MM, Furlong S, Voytek B, Donoghue T, Boettiger CA, Sheridan MA. EEG power spectral slope differs by ADHD status and stimulant medication exposure in early childhood. *J Neurophysiol*. 2019;122(6):2427-2437. doi: 10.1152/jn.00388.2019
29. Tran TT, Rolle CE, Gazzaley A, Voytek B. Linked sources of neural noise contribute to age-related cognitive decline. *J Cogn Neurosci*. 2020;32(9):1813-1822. doi: 10.1162/jocn_a_01584
30. Voytek B, Kramer MA, Case J, et al. Age-related changes in 1/f neural electrophysiological noise. *J Neurosci*. 2015;35(38):13257-13265. doi: 10.1523/JNEUROSCI.2332-14.2015
31. Chini M, Pfeffer T, Hanganu-Opatz I. An increase of inhibition drives the developmental decorrelation of neural activity. *Elife*. 2022;11. doi: 10.7554/eLife.78811
32. Schaworonkow N, Voytek B. Longitudinal changes in aperiodic and periodic activity in electrophysiological recordings in the first seven months of life. *Dev Cogn Neurosci*. 2021;47:100895. doi: 10.1016/j.dcn.2020.100895
33. Martínez-Cañada P, Ness TV, Einevoll GT, Fellin T, Panzeri S. Computation of the electroencephalogram (EEG) from network models of point neurons. *PLoS Comput Biol*. 2021;17(4):e1008893. doi: 10.1371/journal.pcbi.1008893
34. Mazzoni A, Lindén H, Cuntz H, Lansner A, Panzeri S, Einevoll GT. Computing the Local Field Potential (LFP) from integrate-and-fire network models. *PLoS Comput Biol*. 2015;11(12):e1004584. doi: 10.1371/journal.pcbi.1004584
35. Mazzoni A, Panzeri S, Logothetis NK, Brunel N. Encoding of naturalistic stimuli by local field potential spectra in networks of excitatory and inhibitory neurons. *PLoS Comput Biol*. 2008;4(12):e1000239. doi: 10.1371/journal.pcbi.1000239
36. Meghdadi AH, Stevanović Karić M, McConnell M, et al. Resting state EEG biomarkers of cognitive decline associated with Alzheimer's disease and mild cognitive impairment. *PLoS One*. 2021;16(2):e0244180. doi: 10.1371/journal.pone.0244180
37. Vaghari D, Bruna R, Hughes LE, et al. A multi-site, multi-participant magnetoencephalography resting-state dataset to study dementia: the BioFIND dataset. *Neuroimage*. 2022;258:119344. doi: 10.1016/j.neuroimage.2022.119344
38. McKhann G, Drachman D, Folstein M, Katzman R, Price D, Stadlan EM. Clinical diagnosis of Alzheimer's disease: report of the NINCDS-ADRDA work group under the auspices of department of health and human services task force on Alzheimer's Disease. *Neurology*. 1984;34(7):939-944. doi: 10.1212/wnl.34.7.939
39. Shafto MA, Tyler LK, Dixon M, et al. The Cambridge Centre for Ageing and Neuroscience (Cam-CAN) study protocol: a cross-sectional, lifespan, multidisciplinary examination of healthy cognitive ageing. *BMC Neurol*. 2014;14:204. doi: 10.1186/s12883-014-0204-1
40. Albert MS, DeKosky ST, Dickson D, et al. The diagnosis of mild cognitive impairment due to Alzheimer's disease: recommendations from the National Institute on Aging-Alzheimer's Association workgroups on diagnostic guidelines for Alzheimer's disease. *Alzheimers Dement*. 2011;7(3):270-279. doi: 10.1016/j.jalz.2011.03.008
41. Maxfilter Version 2.2. Accessed 18/05/2023, 2023. https://imaging.mrc-cbu.cam.ac.uk/meg/Maxfilter_V2.2
42. Donoghue T, Haller M, Peterson EJ, et al. Parameterizing neural power spectra into periodic and aperiodic components. *Nat Neurosci*. 2020;23(12):1655-1665. doi: 10.1038/s41593-020-00744-x
43. Brunel N, Wang XJ. What determines the frequency of fast network oscillations with irregular neural discharges? I. Synaptic dynamics and excitation-inhibition balance. *J Neurophysiol*. 2003;90(1):415-430. doi: 10.1152/jn.01095.2002
44. Cavallari S, Panzeri S, Mazzoni A. Comparison of the dynamics of neural interactions between current-based and conductance-based integrate-and-fire recurrent networks. *Front Neural Circuits*. 2014;8:12. doi: 10.3389/fncir.2014.00012
45. Linssen C, Lepperød ME, Mitchell J, et al. NEST 2.16.0. Zenodo. 2018. doi: 10.5281/zenodo.1400175
46. Barbieri F, Mazzoni A, Logothetis NK, Panzeri S, Brunel N. Stimulus dependence of local field potential spectra: experiment versus theory. *J Neurosci*. 2014;34(44):14589-14605. doi: 10.1523/JNEUROSCI.5365-13.2014
47. Colclough GL, Brookes MJ, Smith SM, Woolrich MW. A symmetric multivariate leakage correction for MEG connectomes. *Neuroimage*. 2015;117:439-448. doi: 10.1016/j.neuroimage.2015.03.071
48. Lewandowski CT, Maldonado Weng J, LaDu MJ. Alzheimer's disease pathology in APOE transgenic mouse models: the who, what, when,

where, why, and how. *Neurobiol Dis*. 2020;139:104811. doi: 10.1016/j.nbd.2020.104811
49. Cretin B, Sellal F, Philippi N, et al. Epileptic prodromal Alzheimer's disease, a retrospective study of 13 new cases: expanding the spectrum of Alzheimer's disease to an epileptic variant? *J Alzheimers Dis*. 2016;52(3):1125-1233. doi: 10.3233/JAD-150096
50. Vossel KA, Beagle AJ, Rabinovici GD, et al. Seizures and epileptiform activity in the early stages of Alzheimer disease. *JAMA Neurol*. 2013;70(9):1158-1166. doi: 10.1001/jamaneurol.2013.136
51. Sohal VS, Rubenstein JLR. Excitation-inhibition balance as a framework for investigating mechanisms in neuropsychiatric disorders. *Mol Psychiatry*. 2019;24(9):1248-1257. doi: 10.1038/s41380-019-0426-0
52. Lee E, Lee J, Kim E. Excitation/inhibition imbalance in animal models of autism spectrum disorders. *Biol Psychiatry*. 2017;81(10):838-847. doi: 10.1016/j.biopsych.2016.05.011
53. Nelson SB, Valakh V. Excitatory/inhibitory balance and circuit homeostasis in autism spectrum disorders. *Neuron*. 2015;87(4):684-698. doi: 10.1016/j.neuron.2015.07.033
54. Gogolla N, Leblanc JJ, Quast KB, Südhof TC, Fagiolini M, Hensch TK. Common circuit defect of excitatory-inhibitory balance in mouse models of autism. *J Neurodev Disord*. 2009;1(2):172-181. doi: 10.1007/s11689-009-9023-x
55. Varley TF, Sporns O, Puce A, Beggs J. Differential effects of propofol and ketamine on critical brain dynamics. *PLoS Comput Biol*. 2020;16(12):e1008418. doi: 10.1371/journal.pcbi.1008418
56. Lombardi F, Herrmann HJ, de Arcangelis L. Balance of excitation and inhibition determines 1/f power spectrum in neuronal networks. *Chaos*. 2017;27(4):047402. doi: 10.1063/1.4979043
57. Bruining H, Hardstone R, Juarez-Martinez EL, et al. Measurement of excitation-inhibition ratio in autism spectrum disorder using critical brain dynamics. *Sci Rep*. 2020;10(1):9195. doi: 10.1038/s41598-020-65500-4
58. Yang H, Shew WL, Roy R, Plenz D. Maximal variability of phase synchrony in cortical networks with neuronal avalanches. *J Neurosci*. 2012;32(3):1061-1072. doi: 10.1523/JNEUROSCI.2771-11.2012
59. Shew WL, Yang H, Yu S, Roy R, Plenz D. Information capacity and transmission are maximized in balanced cortical networks with neuronal avalanches. *J Neurosci*. 2011;31(1):55-63. doi: 10.1523/JNEUROSCI.4637-10.2011
60. Fingelkurts AA, Kivisaari R, Pekkonen E, Ilmoniemi RJ, Kähkönen S. Local and remote functional connectivity of neocortex under the inhibition influence. *Neuroimage*. 2004;22(3):1390-1406. doi: 10.1016/j.neuroimage.2004.03.013
61. Vaghari D, Kabir E, Henson RN. Late combination shows that MEG adds to MRI in classifying MCI versus controls. *Neuroimage*. 2022;252:119054. doi: 10.1016/j.neuroimage.2022.119054
62. Popescu SG, Whittington A, Gunn RN, et al. Nonlinear biomarker interactions in conversion from mild cognitive impairment to Alzheimer's disease. *Hum Brain Mapp*. 2020;41(15):4406-4418. doi: 10.1002/hbm.25133
63. Monteverdi A, Palesi F, Costa A, et al. Subject-specific features of excitation/inhibition profiles in neurodegenerative diseases. *Front Aging Neurosci*. 2022;14:868342. doi: 10.3389/fnagi.2022.868342
64. van Nifterick AM, Gouw AA, van Kesteren RE, Scheltens P, Stam CJ, de Haan W. A multiscale brain network model links Alzheimer's disease-mediated neuronal hyperactivity to large-scale oscillatory slowing. *Alzheimers Res Ther*. 2022;14(1):101. doi: 10.1186/s13195-022-01041-4
65. Stefanovski L, Meier JM, Pai RK, et al. Bridging scales in Alzheimer's disease: biological framework for brain simulation with the virtual brain. *Front Neuroinform*. 2021;15:630172. doi: 10.3389/fninf.2021.630172
66. Stefanovski L, Triebkorn P, Spiegler A, et al. Linking molecular pathways and large-scale computational modeling to assess candidate disease mechanisms and pharmacodynamics in Alzheimer's disease. *Front Comput Neurosci*. 2019;13:54. doi: 10.3389/fncom.2019.00054
67. Zimmermann J, Perry A, Breakspear M, et al. Differentiation of Alzheimer's disease based on local and global parameters in personalized virtual brain models. *Neuroimage Clin*. 2018;19:240-251. doi: 10.1016/j.nicl.2018.04.017
68. de Haan W, van Straaten ECW, Gouw AA, Stam CJ. Altering neuronal excitability to preserve network connectivity in a computational model of Alzheimer's disease. *PLoS Comput Biol*. 2017;13(9):e1005707. doi: 10.1371/journal.pcbi.1005707
69. Hagen E, Magnusson SH, Ness TV, et al. Brain signal predictions from multi-scale networks using a linearized framework. *PLoS Comput Biol*. 2022;18(8):e1010353. doi: 10.1371/journal.pcbi.1010353
70. Hagen E, Næss S, Ness TV, Einevoll GT. Multimodal modeling of neural network activity: computing LFP, ECoG, EEG, and MEG signals with LFPy 2.0. *Front Neuroinform*. 2018;12:92. doi: 10.3389/fninf.2018.00092
71. Billeh YN, Cai B, Gratiy SL, et al. Systematic integration of structural and functional data into multi-scale models of mouse primary visual cortex. *Neuron*. 2020;106(3):388-403. doi: 10.1016/j.neuron.2020.01.040 e18
72. Schmidt M, Bakker R, Shen K, Bezgin G, Diesmann M, van Albada SJ. A multi-scale layer-resolved spiking network model of resting-state dynamics in macaque visual cortical areas. *PLoS Comput Biol*. 2018;14(10):e1006359. doi: 10.1371/journal.pcbi.1006359
73. Mazzoni A, Brunel N, Cavallari S, Logothetis NK, Panzeri S. Cortical dynamics during naturalistic sensory stimulations: experiments and models. *J Physiol Paris*. 2011;105(1-3):2-15. doi: 10.1016/j.jphysparis.2011.07.014
74. Mazzoni A, Whittingstall K, Brunel N, Logothetis NK, Panzeri S. Understanding the relationships between spike rate and delta/gamma frequency bands of LFPs and EEGs using a local cortical network model. *Neuroimage*. 2010;52(3):956-972. doi: 10.1016/j.neuroimage.2009.12.040
75. Sanz Leon P, Knock SA, Woodman MM, et al. The virtual brain: a simulator of primate brain network dynamics. *Front Neuroinform*. 2013;7:10. doi: 10.3389/fninf.2013.00010
76. Deco G, Senden M, Jirsa V. How anatomy shapes dynamics: a semi-analytical study of the brain at rest by a simple spin model. *Front Comput Neurosci*. 2012;6:68. doi: 10.3389/fncom.2012.00068
77. Destexhe A, Sejnowski TJ. The Wilson-Cowan model, 36 years later. *Biol Cybern*. 2009;101(1):1-2. doi: 10.1007/s00422-009-0328-3
78. El Boustani S, Destexhe A. A master equation formalism for macroscopic modeling of asynchronous irregular activity states. *Neural Comput*. 2009;21(1):46-100. doi: 10.1162/neco.2009.02-08-710
79. Wang XJ. Synaptic basis of cortical persistent activity: the importance of NMDA receptors to working memory. *J Neurosci*. 1999;19(21):9587-9603.
80. Murray JD, Anticevic A, Gancsos M, et al. Linking microcircuit dysfunction to cognitive impairment: effects of disinhibition associated with schizophrenia in a cortical working memory model. *Cereb Cortex*. 2014;24(4):859-872. doi: 10.1093/cercor/bhs370
81. Wang R, Reddy PH. Role of glutamate and NMDA receptors in Alzheimer's disease. *J Alzheimers Dis*. 2017;57(4):1041-1048. doi: 10.3233/JAD-160763
82. Foss-Feig JH, Adkinson BD, Ji JL, et al. Searching for cross-diagnostic convergence: neural mechanisms governing excitation and inhibition balance in schizophrenia and autism spectrum disorders. *Biol Psychiatry*. 2017;81(10):848-861. doi: 10.1016/j.biopsych.2017.03.005
83. Driesen NR, McCarthy G, Bhagwagar Z, et al. The impact of NMDA receptor blockade on human working memory-related prefrontal function and connectivity. *Neuropsychopharmacology*. 2013;38(13):2613-2622. doi: 10.1038/npp.2013.170

84. Fellous JM, Sejnowski TJ. Regulation of persistent activity by background inhibition in an in vitro model of a cortical microcircuit. *Cereb Cortex*. 2003;13(11):1232-1241. doi: 10.1093/cercor/bhg098
85. van Nifterick AM, Mulder D, Duineveld DJ, et al. Resting-state oscillations reveal disturbed excitation-inhibition ratio in Alzheimer's disease patients. *Sci Rep*. 2023;13(1):7419. doi: 10.1038/s41598-023-33973-8

SUPPORTING INFORMATION

Additional supporting information can be found online in the Supporting Information section at the end of this article.

How to cite this article: Martínez-Cañada P, Perez-Valero E, Minguillon J, Pelayo F, López-Gordo MA, Morillas C. Combining aperiodic 1/f slopes and brain simulation: An EEG/MEG proxy marker of excitation/inhibition imbalance in Alzheimer's disease. *Alzheimer's Dement*. 2023;15:e12477. https://doi.org/10.1002/dad2.12477